Two X-ray Sources in 30 Doradus: Wolf-Rayet + Black Hole Binaries?

Q. Daniel Wang
Dept. of Physics & Astronomy, Northwestern University
2145 Sheridan Road, Evanston, IL 60208-3112
Electronic mail: wqd@nwu.edu

ABSTRACT

I report the detection of two X-ray sources of luminosities $\sim 10^{36}$ ergs s^{-1} in the central region of 30 Doradus. These two sources appear point-like in images taken with the *ROSAT* HRI. One of the sources is most likely associated with a close spectroscopic binary R140a2 (WN6) with an orbital period of 2.76 days. The mass of the unknown binary component is likely in the range of $2.4 - 15$ $M_\odot$. This suggests that the X-ray source could represent a long-sought class of binaries containing a Wolf-Rayet star and a black hole. The other source, which coincides spatially with Mk34 (WN4.5), may have a similar nature.

Available X-ray spectral data support this Wolf-Rayet + black-hole binary explanation of the two sources. I have used a *ROSAT* PSPC observation to show that the sources have ultrasoft spectra with possible intrinsic absorption. Modeled with multicolor blackbody disks, the spectra provide estimates of the disks' characteristic inner radii, which are in agreement with those obtained for the known black-hole candidates. An *ASCA* observation has further revealed a hard X-ray spectral component from the central 30 Doradus region. This component, represented by a power law with a photon index of ~ 2.4, may belong to the two sources. The characteristics of both the power-law and ultrasoft components strongly indicates that the two sources are black-hole candidates in high-mass X-ray binaries.

Subject headings: star: Wolf-Rayet — galaxies: Magellanic Clouds — X-rays: general — X-rays: stars

1. Introduction

Although 30 Doradus in the Large Magellanic Cloud (LMC) has been a region of intense interest and study for a long time (Malumuth & Heap 1994 and references therein), detailed X-ray investigations of the region started only recently. Using data from the *Einstein* Imaging Proportional Counter, Wang & Helfand (1991; hereafter WH91) have shown that diffuse hot gas

is the dominant source of X-rays from the region. The hot gas occupies an area of dimension $\sim$ 300 pc around R136, the core of the central cluster NGC 2070 (15 pc = $1'$ at an adopted distance of 51 kpc). But little has yet been found about the discrete X-ray source population in the region. The *Einstein* High Resolution Imager (EHRI) has indicated (only at $\sim 3\sigma$ levels) the presence of two X-ray sources in the central region near R136 (WH91).

To study both the discrete sources and diffuse hot gas in the region, I obtained a deep X-ray image with the *ROSAT* High Resolution Imager (hereafter RHRI; Pfeffermann et al. 1988). This image has led to a firm detection of these two sources and an identification of their probable optical counterparts. I have further extracted information on the sources from the *ROSAT* archive, an *ASCA* spectrum, and various optical observations. I conclude that the two sources are most likely high mass X-ray binaries containing black-hole candidates (HMXB BHCs). In the rest of this paper, I first describe properties of the observations and data analysis, dealing primarily with astrometric problems (§ 2). Then in § 3, results are presented on spatial, spectral, and timing properties of the sources. The nature of the sources is explored by combining information from various observations and by comparing with other X-ray-emitting objects (§ 4). I give a summary in § 5. All statistical uncertainties are quoted at the 90% confidence level.

2. Observations and Data Analysis

While an up-to-date description of *ROSAT* can be found in Briel et al. (1994), I quote here only the most relevant information about the telescope/RHRI system and concentrate on the primary observation (*ROSAT* sequence No. rh600228) used in this work. The observation was targeted at R136 (RA = $5^h38^m43\overset{s}{.}2$; Decl.= $-69°6'0''$ — J2000) and accumulated a total live time of 30153 s over various time segments during 1992 December-10 to 1993 June-14. The field of view of the RHRI system was $\sim 35'$ diameter. The spatial resolution, if characterized by a point-spread function (PSF), was about $6''$ (FWHM) on axis and degraded to $\sim 30''$ at $15'$ off axis. The system had a mean effective area of ~ 80 cm^2, a factor of ~ 10 greater than that of the EHRI, over the 0.65 - 1.9 keV range (where the system's effective area was larger than 20% of its peak value ~ 95 cm^{-2} at ~ 1.1 keV). At $\lesssim 0.5$ keV (i.e., around a second peak of the system's effective area at ~ 0.28 keV), the 30 Doradus contribution can be neglected because of interstellar absorption along the line of sight.

Discrete X-ray sources in the field were detected and analyzed using a maximum likelihood algorithm. This algorithm uses a detection aperture that varies according to the size of the PSF as a function of off-axis angle. Otherwise, the algorithm is very similar to that used in the Standard Analysis Software System (SASS; Downes et al. 1992; Briel et al. 1994).

The aspect error of a *ROSAT* observation is typically a few arcseconds, but occasionally exceeds more than $10''$. I reduced this error in my observation by comparing X-ray and optical

positions of three identified point-like X-ray sources in the field. The optical positions (Table 1) were adopted from the Guide Star Catalog for cal 69 (V = 12) and cal 71 (V = 10), and from Shaerer et al. (1994) for the 50 ms pulsar. This position comparison led to a plate solution, which required shifting the observation 1″ to the west and 3″ to the south from the intended pointing direction, plus a rotation of 0.°42 clockwise around the pointing axis, and gave a mean SASS pixel size of 0.″498. The required rotation agrees with the systematic value $0.°4 \pm 0.°1$ discovered by Kuerster (1993). The mean pixel size is consistent with the value $0.″499 \pm 0.″001$, obtained from a plate solution of an RHRI observation on M31 (Briel et al. 1994 and references therein).

The uncertainty in such a plate solution is primarily systematic. The most important fact that I did not account for is probably the azimuthal asymmetry of the PSF at large off-axis angles. The asymmetry causes a systematic offset of a source centroid (which is the source's detection position) from the source's true position towards the pointing axis. This offset introduces a position error up to $\sim 10''$ near the edges of an observation, although its exact dependance on source off-axis angle has yet to be quantified. The reference sources I used are all at large off-axis angles (Fig. 1 and Table 1). Thus, accounting for the effect would make the mean SASS pixel size smaller ($\sim 0.″001$). Fortunately, the reference sources are located on opposite sides relative to the axis; much of the effect on estimating the shifts and the rotation was canceled in the solution. But one may still expect an error up to $\sim 3''$ in the astrometry of the observation, judging from the differences between X-ray and optical positions (Table 1) and between solutions obtained from selecting different pairs of the reference stars.

Moreover, proper motions of the two Galactic stars may produce position shifts of $\sim 1''$ over a period of ~ 13 yrs between the ESO survey (from which two reference stars' optical positions were derived) and the RHRI observation. For this reason, I compared Guide Star Catalog positions of stars in an Hα image of 30 Doradus (Smith et al. 1992) taken within two years of the X-ray observation, and found no noticeable position deviation ($\lesssim 1''$) of cal 71 relative to other stars in the field. Cal 69 is not in the field of the image, but excluding the star has little effect on the results of the plate solution.

I further corrected for time-dependent aspect errors in the observation. First, for individual observing segments that were separated by more than a hour, I calculated the position centroids of the three brightest sources in the field (i.e., cal 71, 50 ms pulsar, and N157B). Located near the southern edge of the field, cal 69 is not used to avoid effects caused by the spacecraft wobble. I estimated the pointing errors, using a χ^2 fit to the deviations of the source centroids in each individual segment from the sources' mean positions over the entire observation. Only large absolute errors ($\geq 2.″5$) were corrected; those smaller ones were less statistically significant.

Similar astrometric corrections were also made on the RHRI observation (wh500036), which was originally taken by B. E. Aschenbach and was downloaded from the *ROSAT* archive. This observation, pointed at the nearby Crab-like pulsar N157B (Table 1), had a live time of 10910 s. The observation was shifted: 0.″5 to the west, 3.″0 to the south, and 0.°42 clockwise around the

pointing axis, similar to the corrections made on rh600228.

All these astrometric corrections were made directly on the X-ray source positions and on the sky positions of individual RHRI counts before being cast into images (e.g., Figs. 1-3).

To examine physical properties of the two X-ray sources, I extracted spectral data from an observation taken by Y-H. Chu (1993) with the *ROSAT* Positional Sensitive Proportional Counter (PSPC) during 1992 April-29 to May-18. The PSPC had about six independent energy bands over the 0.1 to 2 keV range. For each source, I obtained a spectrum from a pulse height-invariant (PI) channel distribution of net source counts. (The PI binning uses the pulse height energies of individual events recorded by the PSPC and incorporates both the instrument temporal and spatial gain corrections.) The net source counts were obtained from on-source counts from a circle of $0\farcm4$ radius around the source centroid, minus the area-normalized background counts from a concentric annulus with an inner radius of $1\farcm2$ and an outer radius of $2\farcm5$. Vignetting corrections were applied to each of the counts. The contamination from the other source in the background annulus was removed by excluding the area within the source's 90% radius (defined to contain 90% of the counts of a point-like source).

3. Results

Fig. 1 is an overlay of X-ray contours on a digitized ESO plate, illustrating the overall correspondence between X-ray and optical objects in the 30 Doradus region. Fig. 2 is a representation of the X-ray image, optimally smoothed to reveal faint diffuse X-ray features. These two figures confirm the *Einstein* results on the global morphology of diffuse X-rays emanating from the 30 Doradus nebula (WH91); the X-ray-emitting gas is clearly enclosed by filaments, or loops and shells, of warm ionized gas. The wealthy details of the diffuse X-ray component and N157B will be discussed elsewhere. Here, I concentrate on discrete sources in the central region.

3.1. Spatial Properties

Table 1 is a list of point-like sources detected in the 30 Doradus field (Fig. 1). Sources 5 and 7 are the only two sources that show dominant point-like components within the entire nebula above a 5σ source detection threshold of $\sim 3 \times 10^{-3}$ counts s^{-1}. I compared the observed radial intensity profiles of the two sources with the PSF of the RHRI system. χ^2 fits were performed with the normalization of the PSF and the intensity of an assumed uniform local background as two free parameters. Source 5 is consistent with being point-like ($\chi^2/n.d.f. = 15.8/13$), but Source 7 clearly contains a second contribution in addition to a point-like component (28.0/13).

In Figs. 3-4, one can see an intensity excess between $\sim 5''$ - $15''$ off the point-like centroid of Source 7. This excess extends primarily in the direction of R136, covering an area of the greatest massive star concentration in the region. The excess accounts for $\sim 10\%$ of the count rate of the source, corresponding to an *unabsorbed* luminosity of 4×10^{34} ergs s^{-1} in the 0.5 - 2 keV band (see § 3.2). Within a $5''$ radius of R136, stars with a total $L_{bol} \approx 4 \times 10^7 L_\odot$ (Malumuth & Heap 1994), are nominally expected to contribute $0.9 - 5 \times 10^{34}$ ergs s^{-1}, where the lower limit is derived by assuming $L_x(0.5 - 2 \text{ keV})/L_{bol} \approx 6 \times 10^{-8}$ for Wolf-Rayet (WR) stars (Pollock 1987) and the upper limit assuming 3×10^{-7} for O/B stars (Chlebowski 1989). Thus, the excess is consistent with the nominal stellar X-ray contribution in the region, and there is no evidence that R136 contains an exotic X-ray-emitting object.

The centroids of Sources 5 and 7 coincide spatially with R140 and Mk34 (Fig. 3 and Table 1). The optical positions, obtained in a plate solution of the CCD image presented in Fig. 3, are accurate to $\lesssim 1''$ (Parker 1993). Within $\sim 3''$ radii around the centroids (the adopted systematic X-ray position uncertainty), no obvious alternative objects are present as optical counterparts of the X-ray sources. If the position coincidence represents their true physical association with the optical objects, the sources are then the first X-ray detection of WR stars (or systems) outside the Milky Way.

3.2. Spectra and Luminosities

Table 2 summarizes results of model fits to the PSPC spectral data (Fig. 5). All the three spectral models in the table provide satisfactory fits for Source 5, but can be rejected for Source 7 at about the 99% confidence level. As illustrated in Fig. 5b, a couple of line features might be present in the spectrum of Source 7 and are not accounted for by the models. Furthermore, compared to Sources 5, there might be a hard tail in the spectrum of Source 7. This may be explained by the fact that the spectrum includes two components spatially resolved by the RHRI observation (§ 3.1); the tail could be due to relatively hard X rays from normal stars. Nevertheless, the overall spectral shapes of Sources 5 and 7 appear similar, being very steep in the 1-2 keV range and showing cutoffs near 1 keV. The steep spectra are an indication of optically-thick emission from accretion disks (see also § 4). Therefore, among the models included in Table 2, the multicolor blackbody disk (MBD) is probably the most realistic representation of the X-ray spectral data. From the normalizations of the fits with MBD, the inner radii of the disks are derived (Table 3).

The characterization of the X-ray spectra provides the conversion between count rates and energy fluxes of the sources. The *absorbed* energy fluxes of Sources 5 and 7 are 1.2 and 2.3×10^{-13} ergs s^{-1} cm^{-2} in the 0.5 - 2 keV band, which are insensitive to the choice of a specific spectral model. Assuming the best-fit MBD parameters, the luminosities of the two sources are ~ 7 and 6×10^{35} ergs s^{-1} in the 0.5 - 2 keV band.

3.3. Variability

The two X-ray sources are detected in all the three *ROSAT* observations with no evidence of dramatic aperiodic intensity variation, and are therefore not X-ray transients. Only Source 5 showed intensity variation of marginally significance between the two RHRI detections; the mean source count rate during wh500036 was $\sim 2.0 \pm 0.9$ lower than that during rh600228. No significant variability was detected during individual observations. But, owing to the low count rates of the sources, this does not exclude luminosity variations of $\sim 40\%$, for an example, on a timescale of 4000 s for both sources.

There is no evidence for a phase-dependent variation in the intensity of Source 5. A constant intensity fit to the source's RHRI light curve, folded according to the orbital period of R140a2 (see § 4.4), gives $\chi^2/n.d.f = 10.2/8$. The upper limit to the pulse fraction of the source intensity is $\sim 50\%$, assuming a sinusoidal waveform as may be expected from a stellar-wind-driven X-ray source in an eccentric orbit.

4. Nature of the X-ray Sources

Using the *ROSAT* observations, I have shown that two luminous X-ray sources are present in the central region of 30 Doradus. These two sources are most likely associated with WR stars, have X-ray luminosities of $\sim 10^{36}$ ergs s^{-1} in the 0.5-2 keV band, are not X-ray transients, and show steep spectra over the 1-2 keV range and possible intrinsic X-ray absorption. Combining results from an observation made with the *ASCA* X-ray observatory, and information from other wavelength bands, I now attempt to determine the nature of the sources.

4.1. Association with Wolf-Rayet Stars

The association of the two X-ray sources with the WR stars appears to be real. 30 Doradus houses ~ 20 WR stars and ~ 60 O stars of type hotter than O5 in the central diameter of $\sim 3'$ around R136 (e.g., Walborn 1991; Parker 1993). Many of these stars are clustered into groups such as R140 (see § 4.4). Statistically, the chance is small for random position coincidences ($\lesssim 2''$) of the WR stars with the only two X-ray sources in 30 Doradus, and is even smaller for random alignments of the stars with background or foreground objects of comparable or greater X-ray intensities.

The association, if real, provides insight into the nature of the X-ray sources. Since X-rays from individual stars cannot account for the observed source intensities (§ 3.1), the most appealing

model involves accretion-powered compact objects, such as black holes (BHs) or neutron stars. It is believed that most stars near R136 were born during a major star formation burst about 3 ± 1 Myr ago (e.g., Hyland et al. 1992; Lattanzi et al. 1994). Therefore, only the most massive stars ($\gtrsim 50$ $M_\odot$) formed during this episode may have collapsed; the end products are probably BHs if stellar mass BHs do exist and are formed from stars. When such a collapse happens in a massive close binary, the BH is retained in the binary orbit in most cases. Thus, the two X-ray sources may represent HMXBs, most probably WR+BH binaries, which are expected as an evolutionary stage of massive binaries (e.g., Moffat & Seggewiss 1979).

The large X-ray absorption indicated in the spectral fits (Table 2) could be contributed by stellar winds of the WR stars, in addition to the interstellar medium along the lines of sight. Interstellar gas column densities may be estimated from optical extinctions towards R140b and Mk35, whose optical colors, not blended by nearby stars, were measured by Parker (1993). R140b (§ 4.4) has a measured $E(B-V)$ value of 0.12. Mk35, $\sim 10''$ south from both R136 and Mk34 (Malumuth & Heap 1994), has a value of 0.27. From the conversion $N_H/E(B-V) = 2.4 \times 10^{22}$ cm^{-2} mag^{-1} (Fitzpatrick 1985), $N_H \approx 2.9$ and 6.5×10^{21} cm^{-2} for the two stars. Assuming that the stars are located in the same regions as the corresponding X-ray sources, one can then compare the estimated interstellar N_H values with the column densities from the spectral fits (Table 2). For example, the MBD fits suggest considerable amounts of intrinsic absorption ($\gtrsim 2 \times 10^{21}$ cm^{-2}) in both sources. Such intrinsic absorption is expected for wind-driven compact X-ray sources (e.g., Moffat & Seggewiss 1979).

4.2. Accretion Disk Model

WR+BH binaries provide a natural explanation of the observed X-ray properties of the two sources. With their X-ray luminosities $\lesssim 10^{37}$ ergs s^{-1}, the sources are likely driven by material captured from massive winds of the WR stars (Conti 1978). The specific angular momentum in the wind material can result in accretion disks close to the BHs. The disks manifest themselves as ultrasoft components in the X-ray spectra of the sources (e.g., Tanaka & Lewin 1995). The observed steep spectra in the 1-2 keV band do indicate the presence of optically-thick disks, and can be approximately modeled with MBD (Table 3; § 3.2).

In comparison, an HMXB containing a strongly magnetized neutron star ($B \sim 10^{12}$ G) does not normally produce a steep soft X-ray spectrum at a low luminosity state. Because of the strong magnetic field, which is expected for a young neutron star of an age comparable to or smaller than that of R136, no X-ray-emitting accretion disk can be formed. The X-ray emission from the star's surface should have a hard spectrum, typically characterized by a power law of a photon index 1.0-2.0 up to a high energy cutoff at 10-20 keV (e.g., White, Swank, & Holt 1983). This index is significantly smaller than those of Sources 5 and 7 (Table 2). Therefore, the sources do not appear to be neutron star systems.

Assuming MBD, one can estimate the mass M_x of an accreting compact object. If the disk inner radius $R_{in} \sim 3R_s$ (with $R_s = 2GM_x/c^2$ the Schwarzshild radius; Ebisawa et al. 1991 and references therein), where circular orbits become dynamically unstable, $M_x \gtrsim 2.5$ $M_\odot/(\cos\ i)^{0.5}$ for Source 5, and $= 4.3^{+20}_{-3.2}$ $M_\odot/(\cos\ i)^{0.5}$ for Source 7. These mass estimates are probably underestimated due to the oversimplification of the MBD model. The characteristic temperature (T_{in}) at the inner radius of a disk, as given Table 2, is the color temperature rather than the effective temperature, which could be considerably higher (by a factor ~ 1.5; Ebisawa et al. 1991 and references therein). With this effect in the consideration, the estimates of R_{in}, thereof M_x, would be increased by a factor of ~ 2 (Tanaka 1992). Although the theoretical upper limit for a neutron star is ~ 2.5 $M_\odot$ (e.g., Shapiro & Teukolsky 1983), radio observations have constrained masses of neutron stars in binary pulsar systems to be within the limits of 1 and 1.6 $M_\odot$ (e.g., Finn 1994). Thus, the compact objects in Sources 5 and 7 are more likely stellar mass BHs than neutron stars.

Now, let us see whether or not the X-ray luminosities of the sources can be explained by the BH accretion from stellar winds of the WR stars. The bolometric luminosities (L_{bol}) of Sources 5 and 7 are ~ 4 and 1×10^{36} ergs s^{-1}, estimated from the best-fit MBD parameters of each source (Table 2). Further assuming $L_{bol} \approx 0.06\dot{M}c^2$ (Sunyaev & Titarchuk 1980), one can obtain the mass accretion rates ($\dot{M}$) as ~ 10 and 3×10^{-10} $M_\odot$ yr^{-1}. Theoretically, one can expect an accretion rate as

$$\sim (3 \times 10^{-10}\ M_\odot\ \mathrm{yr}^{-1})(\frac{V_{WR}}{3 \times 10^3\ \mathrm{km\ s}^{-1}})^{-4}(\frac{\dot{M}_{WR}}{10^{-5}\ M_\odot\ \mathrm{yr}^{-1}})(\frac{R}{15\ R_\odot})^{-2}(\frac{M_x}{10\ M_\odot})^2, \qquad (1)$$

where V_{WR} and $\dot{M}_{WR}$ are the wind velocity and mass loss rate of a WR star, and R is the distance between a WR star and its BH component (Moffat et al. 1997). Within the uncertainties of the parameters (Usov 1992 and references therein), the wind-driven accretion scenario provides a reasonable explanation of the $\dot{M}$ values of the two sources.

4.3. Comparison with Known Black-Hole Candidates

Table 3 lists parameters of the three previously known HMXB BHCs (Cyg X-1, LMC X-3, and LMC X-1) as well as Sources 5 and 7. The spectrum of an HMXB BHC can be characterized in general by a power law plus an ultrasoft component (e.g., MBD). Normally, the power-law contribution dominates only at energies greater than a few keV (outside the *ROSAT* band), and typically has a photon index of $\sim 2.0 - 2.5$ (e.g., Schlegel et al. 1994; Tanaka & Lewin 1995). Only Cyg X-1 often show a 'low' state in which the spectrum can be reasonably well fitted by a single flatter power law of a photon index ~ 1.5 from ~ 2 to 100 keV (Liang & Nolan 1984; Marshall et al. 1993; Tanaka & Lewin 1995). However, an ultrasoft excess below ~ 2 keV is probably still

required to explain the discrepancy between X-ray-absorbing gas column densities inferred from optical and X-ray measurements (e.g., Balucinska & Hasinger 1991).

The evidence that the two 30 Doradus sources have a power-law component expected for HMXB BHCs comes from a recent *ASCA* observation (Itoh et al. 1994), which is sensitive to the 0.5 - 10 keV range. I have examined images constructed with the observation in different energy bands. Counts in the 2 - 10 keV image strongly concentrate to the central region where the two sources are located (see also Itoh et al. 1994), whereas the image in the 0.5 - 2 keV band shows a count distribution similar to that in Fig. 2. Interestingly, the integrated spectrum of 30 Doradus can be well fitted with two spectral components: an optically-thin thermal plasma and a power law. These results suggest that the thermal plasma contribution, dominating at energies $\lesssim 2$ keV, is overwhelmed by diffuse hot gas, and that the power-law component, important at higher energies, can be explained, at least partially, by the presence of the two sources. The photon index $2.42^{+0.18}_{-0.19}$, given by Itoh et al. (1994), is consistent with the expected value for HMXB BHCs. The luminosity of the power-law component is $\sim 1.4 \times 10^{36}$ ergs s^{-1} in the 0.5 - 10 keV range. Even in the 0.5 - 2 keV range, the power-law contribution of $\sim 8 \times 10^{35}$ ergs s^{-1} may not be negligible, compared to the summed luminosity of Sources 5 and 7 ($\sim 13 \times 10^{35}$ ergs s^{-1}), inferred from the *ROSAT* observations. However, the power-law contribution could have been substantially overestimated. The fit with a plasma of a single temperature is probably an oversimplification; the use of a multi-temperature plasma would reduce the index, thereof the contribution, of the power law in the 0.5 - 2 keV band.

The ultrasoft component of the sources, revealed by the *ROSAT* PSPC spectra, is another important signature of HMXB BHCs (Tanaka 1994). From Table 3, one can find a general correlation between T_{in} and L_x ($\sim L_{bol}$), which roughly agrees with the relation predicted from the MBD model (e.g., Ebisawa et al. 1991):

$$T_{in} \approx 0.6 \text{ keV}(M_x/10 \text{ M}_\odot)^{-0.5}(L_{bol}/10^{38} \text{ ergs s}^{-1})^{0.25}, \quad (2)$$

within the uncertainties of the relevant parameters. This indicates that the ultrasoft spectra of the sources can be explained by their relatively low L_x (or $\dot{M}$) values. The relatively low mass accretion rates of these two sources are expected because they are most likely wind-driven systems, whereas the known HMXB BHCs are powered by Roche-lobe overflows (McClintock 1991 and references therein). Moreover, the R_{in} values of the sources (Table 3) are also consistent with those of other HMXB BHCs. By contrast, low-mass X-ray binary BHCs have $R_{in} \lesssim 10$ km and T_{in} in the range of 1.4 - 1.5 keV (Tanaka & Lewin 1995), incompatible with the parameters obtained for the sources.

It, therefore, appears that the 30 Doradus sources represent an extension of the known HMXB BHCs to low luminosities, and are likely powered by accretion from stellar winds.

4.4. Optical Properties

The positional coincidence of Source 5 with R140 makes the WR+BH binary explanation particularly attractive. R140 is a visual multiple star system. The brightest three stars, which form the north-east elongation as seen in Fig. 3, have been studied both photometrically and spectroscopically by Moffat et al. (1987). R140a1 (WC5) looks brighter than normal, suggesting a possible companion O star. But no variation in the radial velocity (RV) of the WR star has been detected. R140b is likely a single normal WN6 star. Most interesting is R140a2 (WN6), which is a close spectroscopic binary with a period of 2.76 days. The nature of the binary partner is, however, unknown. The optical light curve of the binary shows phase-dependent variations with an amplitude $\gtrsim 0.04$ mag. But the optical colors do not seem to vary. This could be explained by electron scattering effects in the WR wind. From the observed intensity changes and the lack of color variations, Moffat et al. estimated that the orbital inclination i lies in the range of $30^\circ - 70^\circ$. The orbit eccentricity e is also unknown. It is expected to be close to zero if the binary of such a short period contains two normal stars (Cherepashchuk 1991). However, if a supernova happened in the binary, the orbit could be highly eccentric. But, this also depends on whether or not there was considerable amounts of mass ejection during the supernova explosion, and on how effective the tidal evolution may have been in circularizing the orbit (Savonije & Papaloizou 1984). An orbit of large eccentricity should cause a noticeable phase-dependent variation in $\dot{M}$ (§ 4.2), thereof, the source intensity. The lack of such a variation in the observations may indicate $e \sim 0$. Furthermore, from the RV amplitudes of He II λ4686 and N IV λ4058 lines of the WR star, Moffat et al. derived a mass function $f(m) = 0.10$ M$_\odot$.

These estimates of the orbital parameters provide constraints on the mass of the unknown binary partner of R140a2. From the definition of the mass function, I obtain a solution $M_x = M_{WN}/[(M_{WN}/f(m))^{1/3} \sin i - 2/3]$. If the mass of the WN star (M_{WN}) is within the known mass range of WN stars from 8 to 48 M$_\odot$ (Cherepashchuk 1991), the solution gives 2.4 M$_\odot$ $< M_x <$ 15 M$_\odot$, consistent with the mass estimate from the MBD fit to the PSPC spectrum of Source 5 (§ 4.2). Hence, it is reasonably to assume that Source 5 is associated with R140a2 and represents a BHC.

Mk34 does not appear as a visual multiple star system in an *HST* WFC2 image. (R140 has not been observed by the *HST*.) Spectroscopic observations are needed to see whether or not this WR star is also in a close binary system similar to R140a2.

4.5. Alternative Explanation: Colliding Wind Systems?

Could the two X-ray sources be explained as colliding wind systems? Or could the two WR stars be in binaries containing only normal massive stars (e.g., WR+O)? Theoretically, it may be possible to postulate a colliding wind model accounting for an X-ray luminosity of up to $\sim 10^{35}$ ergs s^{-1} (e.g., Luo & McCray 1990; Usov 1992). Observationally, however, there is no

evidence for such a luminous colliding wind system. All WR stars, including binaries, in the Milky Way have their individual X-ray luminosities $\lesssim 10^{34}$ ergs s^{-1} (e.g., Pollock 1987). No other WR star is known as an X-ray source in the LMC (Wang et al. 1991) or in the SMC (Wang & Wu 1992). About 40% of LMC WR stars are in binaries which could be colliding wind systems. A few of these binaries have orbital periods comparable to or smaller than that of R140a2; for instance, HD 36521 (WC4+O6V-III) has a period of 1.9 days (Moffat et al. 1986). The non-detection of these binaries as X-ray sources suggests that colliding wind systems in the LMC cannot be much brighter than their Galactic counterparts. Furthermore, the binary partner of R140a2 is unlikely a normal massive star. The upper bound of M_x is considerably smaller than the expected mass of an O star ($\gtrsim 20$ M$_\odot$). Also for the partner to be an O star, the mass function requires $M_{WN}/M_x \gtrsim 4$, which falls outside the range of 0.17 - 2.67 for all known WR+O binaries (Cherepashchuk 1991). A binary containing two WR stars, or a WR star accompanied by a supergiant, is very rare, since it arises only from a wide pair with very close initial masses of components. Therefore, colliding wind systems do not appear as a viable explanation of the X-ray sources.

5. Summary

ROSAT observations have shown the presence of two X-ray sources in the central region of 30 Doradus. These two sources coincide in position with WR stars to $\lesssim 2''$. One of the WR stars is in a spectroscopic binary system; the unknown binary component with its mass in the range of 2.4 - 15 M$_\odot$ is likely a black hole, accreting from the stellar wind of the star. Both sources show extremely steep spectra and possible intrinsic absorption in the 0.5 - 2 keV range. Modeled with MBD, the spectra give R_{in} as $\gtrsim 22$ for one source and $= 38^{+178}_{-18}$ km/(cos i)$^{0.5}$ for the other. These R_{in} values are comparable to those obtained for the known HMXB BHCs. The ultrasoft characteristics of the spectra with $T_{in} \sim 0.2$ keV is consistent with the relatively low luminosities of the sources ($\sim 10^{36}$ ergs s^{-1}) compared to the known BHCs. At energies $\gtrsim 2$ keV, covered by an *ASCA* observation, there is evidence for the presence of a power-law component with a photon index of ~ 2.4, similar to the values of the HMXB BHCs. Furthermore, the sources do not appear to be transients although aperiodic intensity variability of a factor $\lesssim 2$ cannot be ruled out by the data. These results suggest that the two X-ray sources are WR+BH binaries, most probably wind-driven systems.

The confirmation of the two sources as WR+BH binaries at a known distance of the LMC will have important implications for our understanding of the evolution and mass distribution of massive stars (e.g., the calculation of the initial mass function of 30 Doradus stars; Parker & Garmany 1994; Cherepashchuk 1991 and references therein) as well as for studying accretion processes of compact objects.

There might be similar sources in the Milky Way, especially in recent star formation regions. But, the ultrasoft component of such sources would be difficult to detect because of severe

line-of-sight absorption of soft X rays. In the LMC, the interstellar absorption is relatively smaller, partly because of the lower metallicity of gas in the Cloud. Therefore, it is easier to detect sources with ultrasoft spectra in the LMC than in the Milky Way.

I thank J. Parker for providing the CCD image and astrometry information, A. F. J. Moffat for commenting on optical observations of Wolf-Rayet stars, and the referee for comments toward the improvement of this paper. I am grateful to G. S. Miller and R. Taam for discussing the black-hole scenario and for commenting on an early version of the paper. This work was supported by the Lindheimer Fellowship and NASA grant NAG5-2717.

Table 1
ROSAT **HRI Detections of Discrete X-ray Sources in the 30 Doradus field**[a]

Source No.	RA (X-ray)	Decl. (X-ray)	RA (optical)	Decl. (optical)	HRI Rate (counts ks^{-1})	ID	Comments and References[b]
1	$5^h37^m47\overset{s}{.}6$	-69°10′20″			52.5 ± 1.4	SNR N157B	p(?)+d, [1]
2	5 38 10.2	-68 57 01			2.5 ± 0.5		p
3	5 38 16.7	-69 23 32	5 38 16.3	-69 23 34	42.6 ± 1.6	cal 69	p, Galactic star, dK7e, [2]
4	5 38 34.7	-68 53 07	5 38 34.6	-68 53 07	69.5 ± 1.8	cal 71	p, Galactic star, G2V, [2]
5	5 38 41.8	-69 05 14	5 38 41.7	-69 05 13.5	5.1 ± 0.5	R140	p, WR, [3] [4]
6[c]	5 38 44.0	-68 52 42			10.9 ± 0.9		p
7	5 38 44.4	-69 06 07	5 38 44.3	-69 06 05.3	8.1 ± 0.6	Mk34	p+d, WN4.5, [3] [4]
8	5 40 11.1	-69 19 55	5 40 11.0	-69 19 55.2	239.9 ± 3.2	SNR N158	p+d, 50ms pulsar, [5] [6]

[a]The equinox of the positions is J2000. Peaks that represent intensity enhancements of diffuse X-ray features are not included. The optical positions should be accurate to within $\sim 1''$. The uncertainties in the X-ray positions are primarily systematic, ranging from $\lesssim 3''$ on axis to $\sim 10''$ at $\sim 15'$.

[b]A letter "p" (or "d") indicates the presence of a point-like (or diffuse) component of a source. References are for optical positions and IDs: [1] Dickel et al. 1993; [2] Cowley et al. (1984); [3] Moffat et al. (1987); [4] Parker (1993); [5] Shearer et al. (1994) ; [6] Seward & Harnden Jr. (1994).

[c]The count rate is uncertain because of confusion with Source 4.

Table 2
Source Spectral Parameters[a]

Model	T (keV) or α		N_H (10^{22} cm^{-2})		χ^2
			Source 5		
BB	0.11	(0.05, 0.18)	1.3	(0.4, 3.6)	12
MBD	0.13	(0.10, 0.21)	1.2	(0.5, 2.0)	12
PL	10	($\geq$ 6.5)	2.0	($\geq$ 1.8)	12
			Source 7		
BB	0.21	(0.15, 0.32)	1.2	(0.54, 1.9)	35
MBD	0.24	(0.17, 0.35)	1.4	(0.95, 2.1)	35
PL	5.6	(3.2, 9.0)	1.8	(1.0, 3.1)	34

[a]Parameters were included for three spectral models: black-body (BB), multicolor blackbody disk (MBD; Pringle 1981; Makishima et al. 1986), and power law (PL). α is the photon index of a power law. N_H is the equivalent hydrogen column density of X-ray-absorbing gas with assumed metal abundances as 40% of the solar values (Meyer et al. 1994; de Boer et al. 1985; Morrison & McCammon 1983). Parameter limits are all at the 90% confidence level. The number of degrees of freedom in the spectral fits is 17 (Source 5) and 18 (Source 7).

Table 3
Comparisons of Black-Hole Candidates[a]

Source	Source 5	Source 7	Cyg X-1	LMC X-3	LMC X-1
Orbital Period (d)	2.8	–	5.6	1.7	4.2
f(m) ($M_\odot$)	0.10	–	0.25	2.3	0.14(?)
Companion	WN6	WN4.5	O9.7Iab	B3V	O7-9III(?)
Transient	no	no	no	no	no
L_x(ergs s^{-1})	$\sim 10^{36}$	$\sim 10^{36}$	$\sim 2 \times 10^{37}$	$\sim 4 \times 10^{38}$	$\sim 2 \times 10^{38}$
T_{in} (keV)	0.10-0.21	0.17-0.35[b]	~ 0.38	~ 1.1	~ 0.83
$R_{in}(\cos i)^{0.5}$ (km)	$\gtrsim 22$	10-216	18-30 (D/2.5 kpc)	~ 24	~ 40

[a]Parameters for Cyg X-1, LMC X-1, and LMC X-3 are from Ebisawa et al. (1991), Schlegel et al. (1994), Tanaka (1994), and Tanaka & Lewin (1995). The candidacy of LMC X-1 is somewhat questionable (Tanaka & Lewin 1995 and references therein). X-ray luminosities are estimated roughly in 1.2 - 10 keV range. Optical parameters for Sources 5 and 7 are from Moffat et al. (1986). The values of $R_{in}(\cos i)^{0.5}$, where R_{in} and i are the inner radius and inclination angle of an accretion disk, are obtained from spectral fits with the multicolor blackbody disk model (Makishima et al. 1986; Ebisawa et al. 1991).

[a]Probably overestimated because of the spectral contamination from R136 (§ 3.2).

REFERENCES

Balucinska, M., & Hasinger, G. 1991, A&A, 241, 439

Briel, U. G., et al. 1994, *ROSAT* User's Handbook

Cherepashchuk, A. M. 1991, Wolf-Rayet Stars and Interrelations with Other Massive Stars in Galaxies (IAU Symp. No. 143), Ed. K. A. van der Hucht & B. Hidayat, (Kluwer Academic Pub), p187

Chiappetti, L., et al. 1985, Sp. Sci. Rev., 40, 207

Chlebowski, T. 1989, ApJ, 341, 427

Lattanzi, M. G., et al. 1994, ApJL, 427, 21

Chu, Y-H. 1993, The Soft X-ray Cosmos, AIP Conf. Proc. 313, (AIP, New York), ed. E. M. Schlegel, & R. Petre, p. 154

Conti, P. S. 1978, A&A, 63, 225

Cowley, A. P., et al. 1984, ApJ, 286, 196

de Boer, K. S., Fitzpatrick, E. L., & Savage, B. D. 1985, MNRAS, 217, 115

Dickel, J. R., et al. 1994, AJ, 107, 1067

Downes, R., et al. 1994, The *ROSAT* Data Products Guide

Ebisawa, K., et al. 1991, ApJ, 367, 213

Finn, L. S. 1994, Phys. Rew. Let., 73, 1878

Fitzpatrick, E. L. 1985, ApJ, 299, 219

Hyland, A. R., et al. 1992, MNRAS, 257, 391

Itoh, M., et al. 1994, New Horizon of X-ray Astronomy, ed. F. Makino, & T. Ohashi, (Tokyo: Universal Academy Press), p507

Kuerster, M. 1993, *ROSAT* Status Report, No. 67

Lattanzi, M. G., et al. 1994, ApJL, 427, 21

Liang, E. P., & Nolan, P. L. 1984, Sp. Sci. Rev., 38, 353

Luo, D., & McCray, R. 1990, ApJ, 360, 267

Makishima, K., et al. 1986, ApJ, 308, 635

Malumuth, E. M., & Heap, S. R. 1994, AJ, 107, 1054

Marshall, F. E., et al. 1993, ApJ, 419, 301

McClintock, J. E. 1991, Relativistic Astrophysics, Cosmology and Fundamental Physics, ed. J. D. Barrow et al., (New York: The New York Academy of Science), 647, 496

Meyer, D. M., et al. 1994, ApJL, 437, 59

Moffat, A. F., & Seggewiss, W. 1979, A&A, 77, 128

Moffat, A. F., et al. 1986, AJ, 91, 1386

Moffat, A. F., et al. 1987, ApJ, 312, 612

Morrison, R., & McCammon, D. 1983, ApJ, 270, 119

Parker, J. Wm. 1993, AJ, 106, 560

Parker, J. Wm. & Garmany, C. D. 1994, AJ, 106, 1471

Pfeffermann, E., et al. 1988, Proc. SPIE, 733, 519

Pollok, A. M. T. 1987, ApJ, 320, 283

Pringle, J. 1991, ARA&A, 19, 137

Savonije, G. J., & Papaloizou, J. C. B. 1984, MNRAS, 207, 685

Seward, F. D., & Harnden, Jr., F. R. 1994, ApJ, 421, 581

Shapiro, S., & Teukolsky, S. 1983, Black Holes, White Dwarfs, and Neutron Stars (New York: Wiley)

Shearer, A., et al. 1994, ApJL, 423, 51

Schlegel, E. M., et al. 1994, ApJ, 422, 243

Smith, R. et al. 1992, An image taken at CTIO and installed in Internet by T. Ingerson

Sunyaev, R. A., & Titarchuk, L. G. 1980, A&A, 86, 121

Tanaka, Y. 1992, Ginga Memorial Symp., ed. F. Makino, & F. Nagase, p. 19

Tanaka, Y., & Lewin, W. H. G. 1995, X-rat Binaries, ed. W. H. G. Lewin, J. van Paradijs, & E. P. J., van den Heuvel, (Cambridge: Cambridge Univ Press), in press

Tanaka, Y. 1994, New Horizon of X-ray Astronomy, ed. F. Makino, & T. Ohashi, (Tokyo: Universal Academy Press), p37

Usov, V. V. 1992, ApJ, 389, 635

Wang, Q. D., Hamilton, T. T., Helfand, D. J., & Wu, X. 1991, ApJ, 374, 475

Wang, Q. D., & Wu, X. 1992, ApJS, 78, 391

Wang, Q. D., and Helfand, D. J. 1991, ApJ, 370, 541

White, N. E., Swank, J. H., Holt, S. S. 1983, ApJ, 270, 711

Wolborn, N. R. 1991, Massive Stars in Starbursts, ed. C. Leitherer, et al. (Cambridge: Cambridge University Press), p. 145

Figure Captions

Fig. 1: 30 Doradus region in X ray and optical. Contours of X-ray intensity, smoothed with a Gaussian of FWHM = $18''$, are at 2.5, 4, 7, 12, 20, 40, 80, and 160σ ($1\sigma = 1.0 \times 10^{-3}$ counts s^{-1} arcmin^{-2}) above a local background of 5.6×10^{-3} counts s^{-1} arcmin^{-2}. The gray-scaled image is a representation of a digitized ESO survey blue plate taken on December-3, 1979.

Fig. 2: X-ray image of 30 Doradus. The image is adaptively smoothed with a Gaussian of adjustable size to achieve a constant local count-to-noise ratio of ~ 8 over the image. The contours are at 3, 4, 6, 9, 13, 18, 24, 31, 40, 50, 100, 200, 400, and 800σ ($1\sigma = 5.0 \times 10^{-4}$ counts s^{-1} arcmin^{-2}) above a local background of 5.3×10^{-3} counts s^{-1} arcmin^{-2}.

Fig. 3: Central region of 30 Doradus in X ray and optical. The X-ray intensity is a coadd of the two RHRI images and is smoothed with a Gaussian of FWHM= $4''$. The lowest contour is 3σ ($1\sigma = 1.93 \times 10^{-3}$ counts s^{-1} arcmin^{-2}) above a background level of 6 $\times 10^{-3}$ counts s^{-1} arcmin^{-2}; the intensity increment of each subsequent contour is 1.5 times the previous one. The optical CCD image was gray-scaled logarithmically. The astrometry of the plate, corrected with star positions in Parker (1993), should be better than $\sim 1''$.

Fig. 4: RHRI radial intensity distributions of Sources 5 (*triangles*) and 7 (*squares*), compared to the expected PSF of the RHRI system (solid curve).

Fig. 5: *ROSAT* PSPC spectra of Sources 5 (a) and 7(b), together with the best fits of the multicolor blackbody disk model (Table 2).

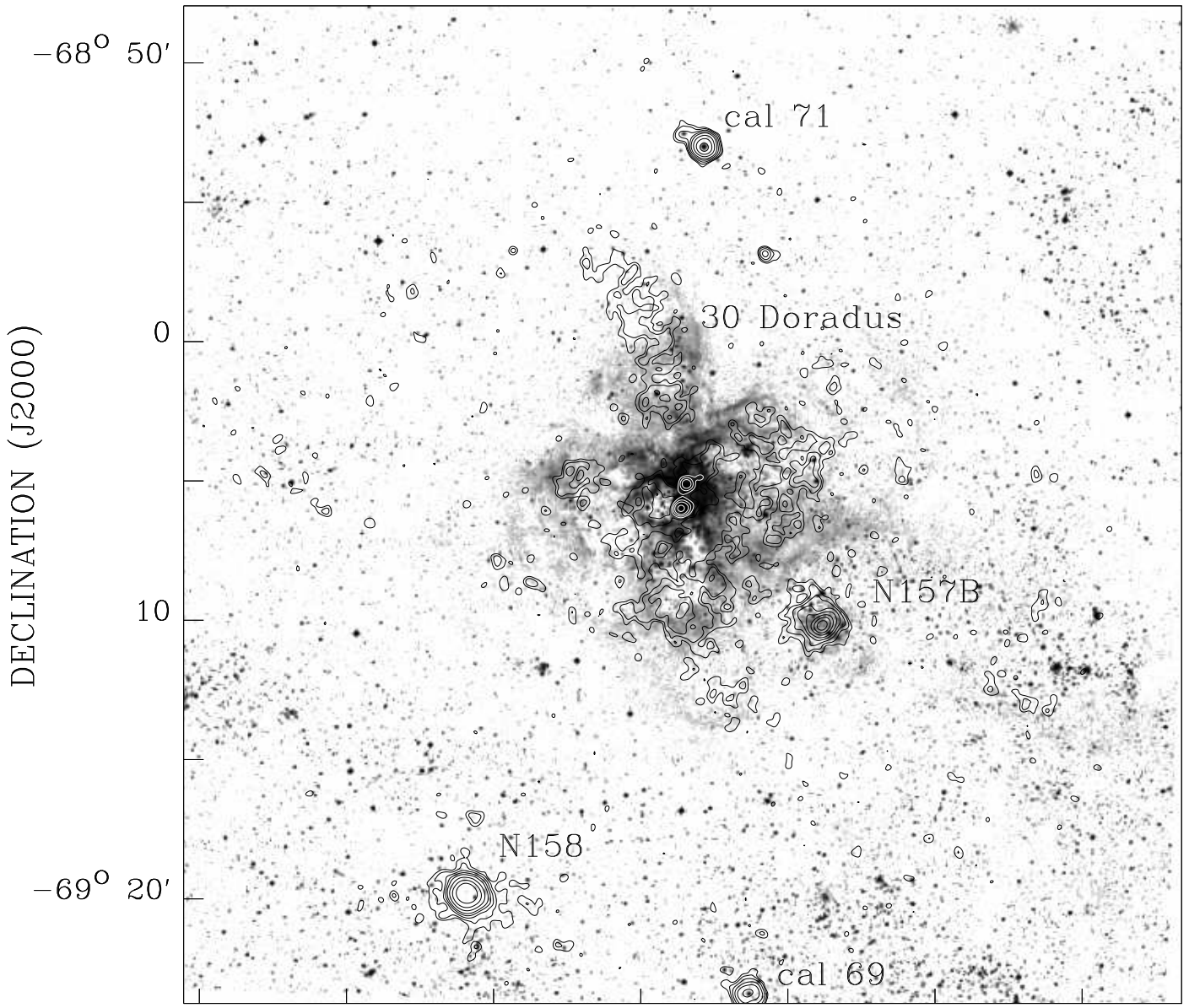

IMAGE SIZE

X: 720

Y: 720

MIN: −5001.0000

MAX: 13876.891

26−Jan−1995 08:42

CONTOUR LEVELS:

0:	8.14000
1:	9.64000
2:	12.6400
3:	17.6400
4:	25.6400
5:	45.6400
6:	85.6400
7:	165.640

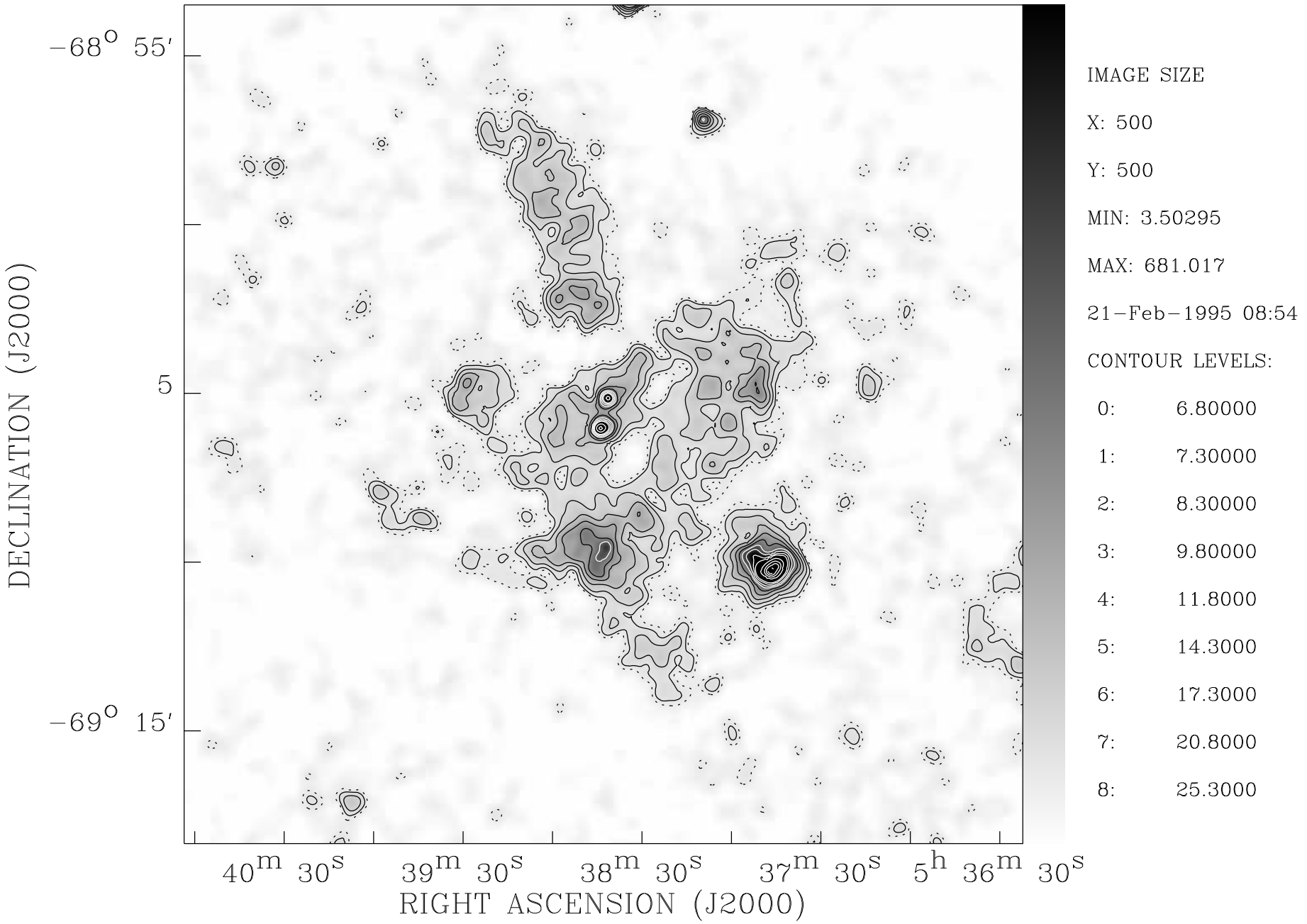
−68° 55′
5
−69° 15′
DECLINATION (J2000)
40m 30s
39m 30s
38m 30s
37m 30s
5h 36m 30s
RIGHT ASCENSION (J2000)
IMAGE SIZE
X: 500
Y: 500
MIN: 3.50295
MAX: 681.017
21−Feb−1995 08:54
CONTOUR LEVELS:
0: 6.80000
1: 7.30000
2: 8.30000
3: 9.80000
4: 11.8000
5: 14.3000
6: 17.3000
7: 20.8000
8: 25.3000

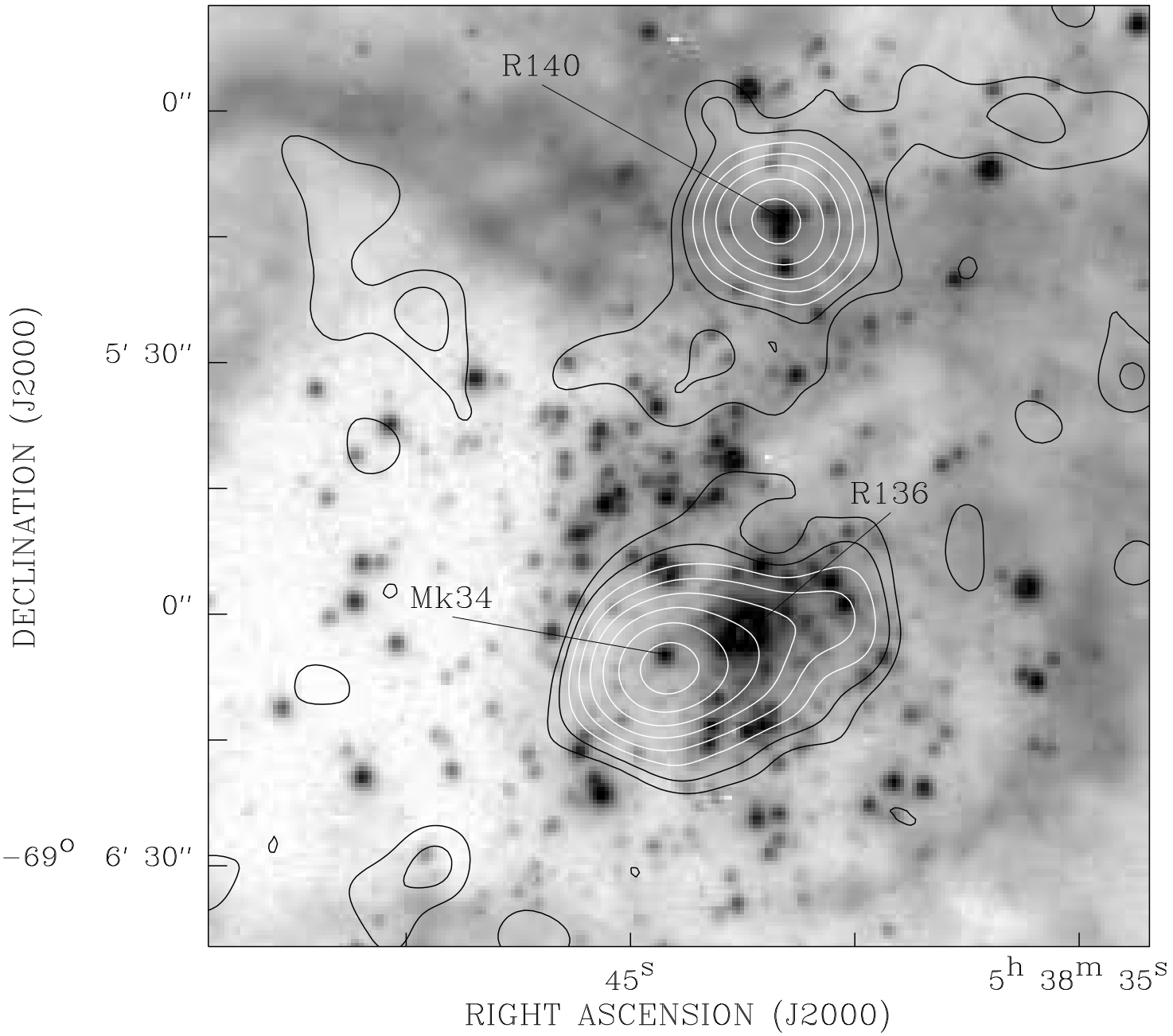
R140
R136
Mk34
0″
5′ 30″
0″
−69° 6′ 30″
DECLINATION (J2000)
45s
5h 38m 35s
RIGHT ASCENSION (J2000)

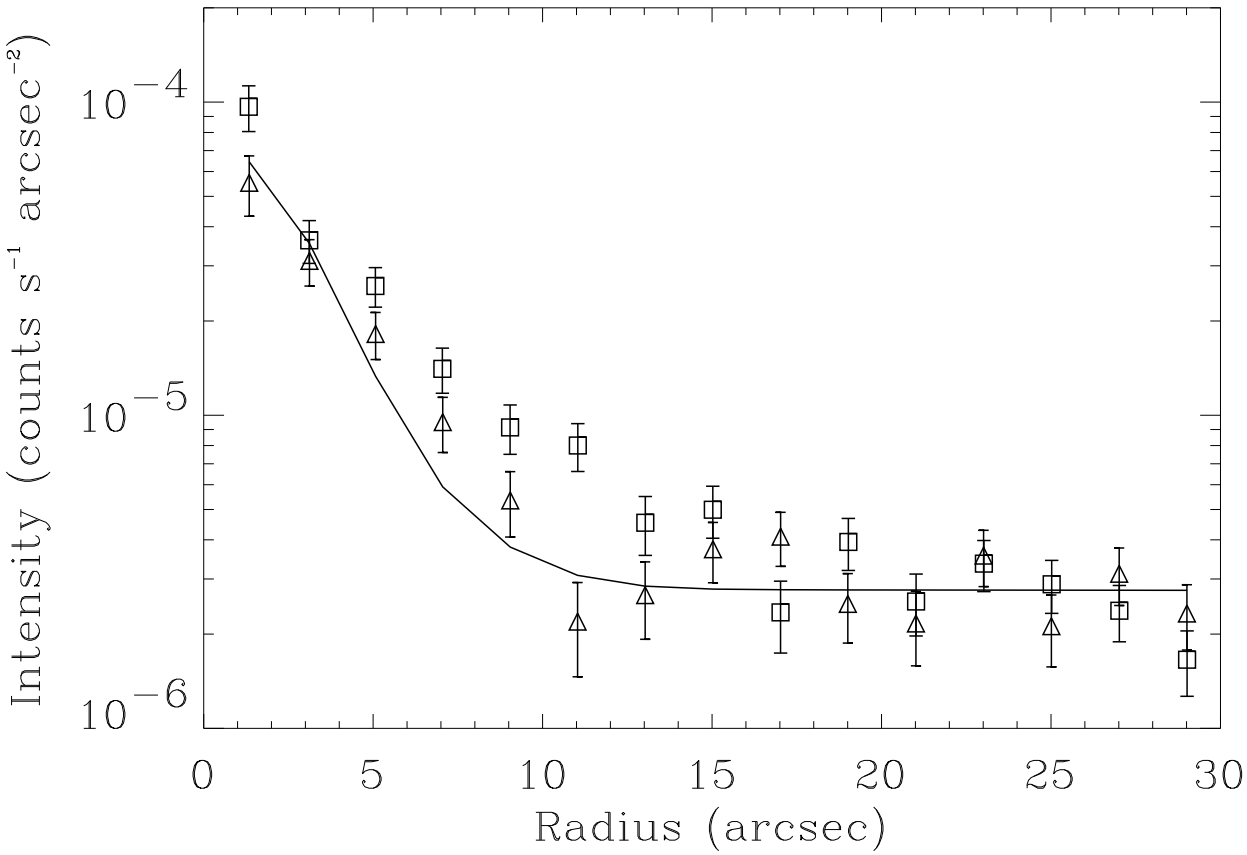
Intensity (counts s^{-1} arcsec^{-2})
10^{-4}
10^{-5}
10^{-6}
0
5
10
15
20
25
30
Radius (arcsec)

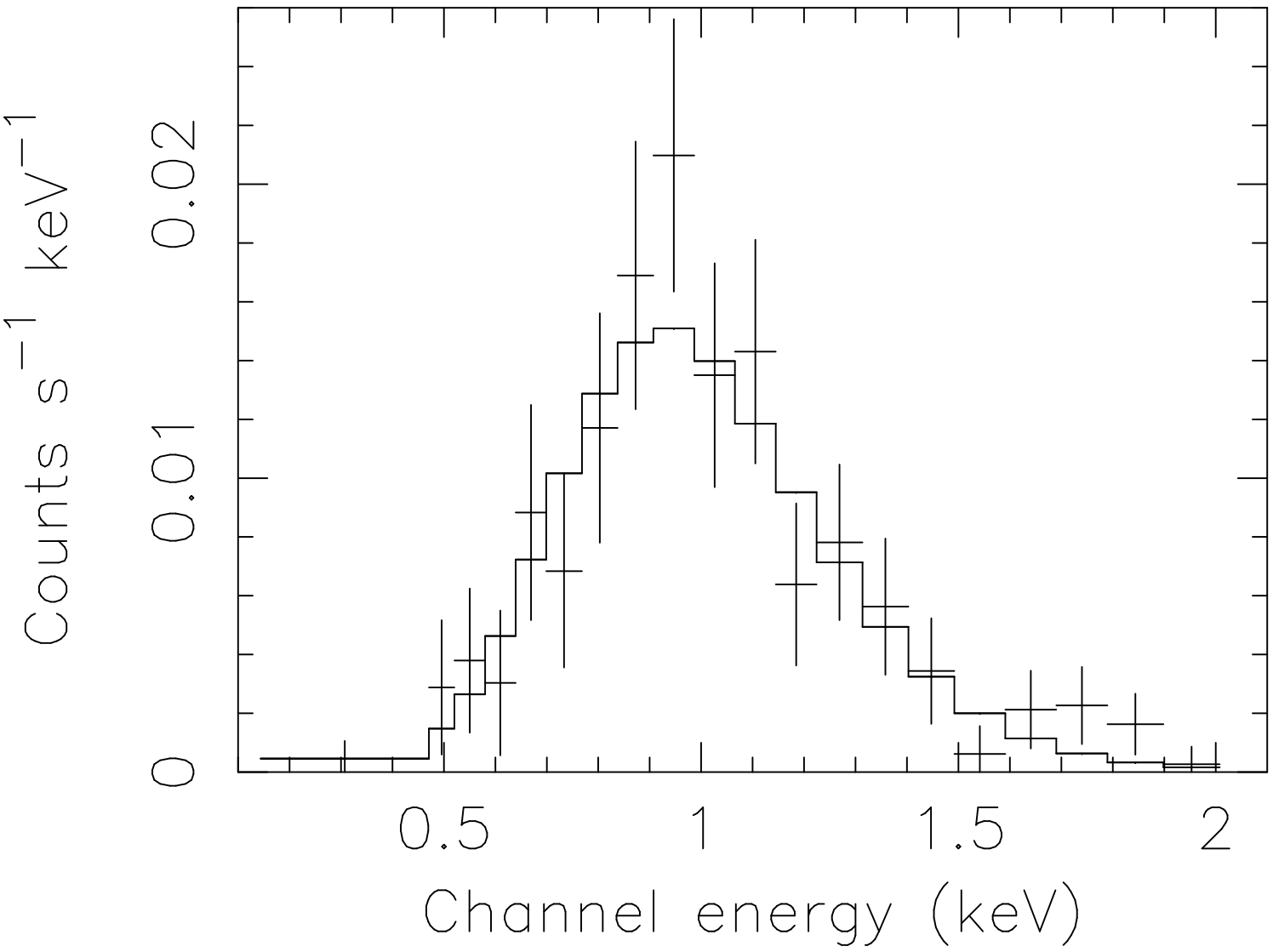

wqd 16-Mar-1995 08:30

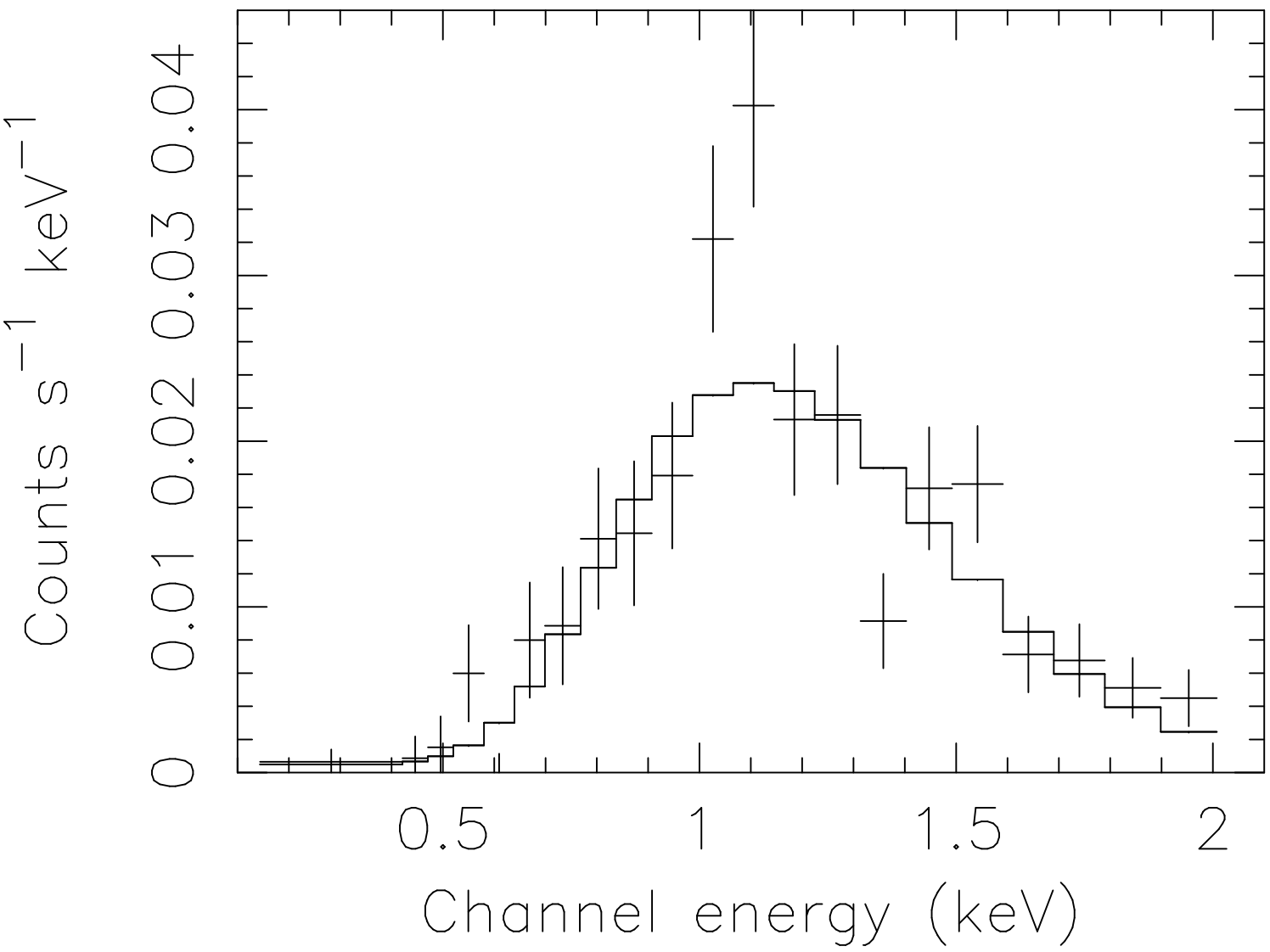

wqd 16-Mar-1995 11:42